Radiation Physics and Chemistry 236 (2025) 112904

Contents lists available at ScienceDirect

Radiation Physics and Chemistry

journal homepage: www.elsevier.com/locate/radphyschem

Dosimetric evaluation of 6 MV photon beams in small fields using PRIMO-penEasy Monte Carlo

Nataly Díaz [a,*], Amaia Villa Abaunza [a], Jorge Muñoz [c], José Manuel Udías [a,b], Paula Ibáñez [a,b]

[a] Nuclear Physics Group and IPARCOS, Department of Structure of Matter, Thermal Physics and Electronics, CEI Moncloa, Universidad Complutense de Madrid, Madrid, 28015, Spain
[b] Instituto de Investigación Sanitaria del Hospital Clínico San Carlos, Madrid, 28011, Spain
[c] San Ignacio University Hospital, Pontificia Universidad Javeriana, Bogotá D.C., 110311, Colombia

ARTICLE INFO

Handling Editor: Dr. Chris Chantler

Keywords:
Elekta
PRIMO MC
Radiochromic films EBT3
Semiflex ionization chamber

ABSTRACT

Dosimetric validation of clinical radiotherapy plans for small fields requires high-precision instrumentation to ensure accuracy and spatial resolution. This study proposes a combination of PRIMO and penEasy Monte Carlo simulators to address scenarios where direct measurements are impractical, challenging, or yield inconsistent results due to detector limitations.

We compared three dosimetric tools: A Semiflex ionization chamber PTW (model 31010) within a water-filled acrylic tank; EBT3 radiochromic films positioned between solid water layers; and PRIMO-PenEasy simulations. Experiments were performed at San Ignacio University Hospital in Bogota, Colombia, with dose measurements in two small fields and one conventional field for an Axesse-type linear accelerator.

Results indicate that EBT3 radiochromic film show better agreement with MC simulation than the Semiflex ionization chamber, likely due to the chamber dose averaging effect across its detection volume. Additionally, variations in off-axis ratios were noted in both crossplane and inplane directions with more pronounced discrepancies observed in small fields compared to the conventional field. Overall, PRIMO-PenEasy MC simulations demonstrated accurate dose distributions and can be used as a viable for dosimetric validation in small photon fields.

1. Introduction

The increase of cases treated with stereotactic radiosurgery (SRS) and intensity-modulated radiation therapy (IMRT), especially for small tumors, has spurred advances in the use of small static fields (Almond et al., 1999) (Leksell, 1983). This progress has been enabled by the adoption of the new TRS-483 protocol for small field dosimetry (Palmans et al., 2017a) and the widespread availability of Multi-Leaf Collimators (MLCs). These advances have lead to exploring the application of small treatment field sizes in equipments originally designed for conventional pho-ton fields. However, small fields introduce specific challenges that must be addressed: lack of lateral electronic equilibrium, partial occlusion of the source, disruption of particle fluence within the medium, and signal degradation (Aspradakis et al., 2010) (McNiven et al., 2006). These factors complicate the dose measurements interpretation, making the selection of appropriate detectors essential to avoid dosimetric errors (Ezzell et al., 2009) (Sánchez-Doblado et al., 2003).

For accurate dosimetry, both in the penumbra region and at the central axis, small volume detectors with minimal energy and dose rate dependencies are necessary. Many studies (Palmans et al., 2017a) (McNiven et al., 2006) (Das et al., 2008) (Francescon et al., 1998) have been done about the different types of detectors in small field dosimetry. While ionization chambers (IC) are most commonly preferred in clinical practice, due to their minimal energy dependency in radiotherapy ranges (Gonzalez-Lopez et al., 2015a), their relatively large size can cause dose underestimation of small fields due to dose averaging (Ardila, 2000). An alternative is radiochromic films, which offer high spatial resolution and energy-independent dose response (Chiu-Tsao et al., 2005) (Butson et al., 2006) although their accuracy relies on strict protocols for handling, reading, and analysis (Devic et al., 2016) (Vera, 2018).

* Corresponding author.
E-mail addresses: natadi02@ucm.es (N. Díaz), amavil01@ucm.es (A. Villa Abaunza), jemunozbr@gmail.com (J. Muñoz), jose@nuc2.fis.ucm.es (J.M. Udías), pbibanez@ucm.es (P. Ibáñez).

https://doi.org/10.1016/j.radphyschem.2025.112904
Received 7 January 2025; Received in revised form 18 April 2025; Accepted 3 May 2025
Available online 12 May 2025

Monte Carlo (MC) simulations provide invaluable information during the study of small field radiotherapy (Cheng et al., 2007). PENELOPE (Baro et al., 1995) is one of the most accurate radiation transport MC codes for estimating the dose distribution (Castellano et al., 2007). It requires detailed information on the accelerator's geometry and materials - data often proprietary to the manufacturer. To overcome this limitation, PRIMO was developed (Rodriguez et al., 2013) as a MC code specially designed for radiotherapy, based on PENELOPE. It incorporates the geometrical and physical models of most of Elekta's linear accelerators. PRIMO only requires the user to specify the initial electron beam characteristics, the treatment field size parameters and MLC specifications (Sarin et al., 2020). The software models the accelerator head from the primary electron beam's interaction on the target to the particle interactions with the collimation and MLC systems (Efendi et al., 2020), storing particle information in a phase space (PHSP) file. This file can be used to study small field photon beam characteristics including fluence and energy distributions, dispersion relations, depth-dose curves, and dose profiles. A limitation of PRIMO is the large simulation times required on conventional computers. For instance, simulating 10^9 histories from a standard linear accelerator on a single CPU with 8 GB of RAM and 8 cores may take several weeks. To address this, PRIMO can be combined with penEasy, a general purpose MC code that simulates the transport of electrons, photons, and positrons within an energy range from 50 eV to 1 GeV (Sempau et al., 2011). PenEasy can be installed and executed in a cluster of computers, and PRIMO-generated PHSP files can be used to compute dose distributions in the computating cluster, reducing simulation time from several weeks to hours.

In recent years, some studies have been conducted to evaluate PRIMO MC predictions for small field dosimetry (Sarin et al., 2020) (Efendi et al., 2020). These studies, however, largely rely on comparisons with ionization chambers, which, as mentioned, often suffer from limited spatial resolution. This highlights the need to extend these investigations by including measurements with radiochromic films, which provide superior spatial dose resolution, particularly suited for small field applications. Furthermore, current studies usually do not include fields smaller than $4 \times 4\ cm^2$, revealing a significant limitation in PRIMO MC's validation.

Overcoming this limitation could establish PRIMO MC as a dependable tool in radiotherapy, thereby enabling a more precise resolution of discrepancies observed across various detector types used in small field dosimetry.

Thus, the aim of this study was to evaluate the potential of PRIMO as an alternative tool for small field dosimetry. We conducted dosimetric measurements for photon beams with small field sizes of 2×2 and 4×4 cm^2, along with a standard $10 \times 10\ cm^2$ field, and compared them with PRIMO-penEasy simulations. On the one hand, measurements with a PTW type 31010 ionization chamber (IC) and EBT-3 radiochromic films were performed at San Ignacio University Hospital (Bogota, Colombia) using an Elekta Axesse linear accelerator. On the other hand, simulations of the Elekta Axesse model were performed in PRIMO, using its built-in geometry for the same field sizes. PHSP files generated in PRIMO were then incorporated in penEasy to obtain dose distributions in a water phantom. Measured and simulated doses were compared through mean relative difference, output factors (OF) and gamma analysis (Low et al., 1998).

2. Materials and methods

2.1. Elekta Axesse accelerator

The medical accelerator used in this study was an Elekta Axesse linear accelerator (LINAC) with a photon beam energy of 6 MV. This accelerator is equipped with a beam modulator collimation system that includes a conical primary collimator, a flattening filter and a secondary MLC system made up of 40 pairs of opposing and intertwined tungsten leaves. This configuration allows for the programming of fields in different symmetrical and asymmetrical sizes (Esposito et al., 2018). The leaves move linearly, which can lead to penumbra variations as the leaves move to different positions relative to the central axis (Ardila, 2000).

2.2. Measurements

2.2.1. PTW semiflex 31010 ionization chamber

Percent depth dose (PDD) distributions, crossplane and inplane profiles were measured with PTW Semiflex IC (type 31010) with a 0.125 cm^3 internal cavity volume, positioned within a MP3-M scanning system with $50.0 \times 50.0 \times 40.8\ cm^3$ range. Data analysis was performed using the MEPHYSTO mc^2 software and the step-by-step scanning and CAX correction method were used for centering the IC (Cheng et al., 2007).

For the three field sizes (2×2, 4×4 and $10 \times 10\ cm^2$), dose profiles were measured maintaining an Source to Surface Distance (SSD) of 90 cm and taking into account the camera correction for the effective measurement point. IC readings were corrected for pressure, temperature and polarity. For uncertainty analysis, the TRS 483 code and the dosimetric quantities formalism proposed by Dufreneix et al. (2021) were followed. The percentage variation in dose (ΔD) was obtained from the first measured profile (cross-plane and in-plane). To evaluate detector positioning in x,y, a field size was selected and the standard deviation of the averages of three detector readings for 100 UM in each field was calculated, applying corrections for pressure, temperature, and the correction factors specified in TRS 483 (Palmans et al., 2017b). Finally, the combined uncertainty for each field size was determined, following the methodology of (Dufreneix et al., 2021) with an uncertainty factor ($k = 2$).

The OF for small fields were experimentally measured in accordance with the TRS-483 protocol (Palmans et al., 2017b) for the $2 \times 2\ cm^2$ and the $4 \times 4\ cm^2$ field sizes. The values were normalized to the $10 \times 10\ cm^2$ field. The chamber was placed at a depth of 10 cm in the automatic tank with an SSD of 90 cm, and 100 monitor units (MU) were supplied. Thus, equation (1) was used:

$$OF(i) = \frac{D_{10}(i)}{D_{10}(i)} \tag{1}$$

Where D10 (i) is the measured dose in water at a 10 cm distance for the field i and D10(10) is the dose in water measured for the reference field size of $10 \times 10\ cm^2$. The OF uncertainty was calculated according to equation (1), considering that each term has an associated uncertainty arising from various contributions. The uncertainty estimation is expressed as the combined uncertainty, where each term involves variables previously described in the document, with the correction factors of the TRS 483 code (Palmans et al., 2017b) applied as part of the methodology outlined in (Dufreneix et al., 2021),including an uncertainty factor ($k = 2$).

2.2.2. Gafchromic EBT3 films

Gafchromic EBT3 films (lot No. 2004744) were also used for this study to examine in greater detail the penumbra region and dose fall-off, as they pro-vide higher spatial resolution than the ionization chamber. The films were previously calibrated with doses ranging from 0 to 3 Gy in increments of 0.380 Gy.

To determine dose maps, films were irradiated at field sizes of 2×2, 4×4 and $10 \times 10\ cm^2$ with 400 MU. The phantom consisted of three solid water blocks, each 5 cm thick and $30 \times 30\ cm^2$ in dimension. The films were inserted between the first two slabs, at 5 cm and at 10 cm depth, respectively, for the 6 MV photon beam, maintaining an SSD of 90 cm. Scanning was performed 48 h after irradiation using an Epson 10000XL flatbed scanner in transmission mode with 75 pixels per inch and 16 bits per color channel. The films dose response was carried out

using only the red channel due to the film's higher sensitivity in the red region of the spectrum (Micke et al., 2011). Uncertainty analysis was performed according to Devic et al. (2004).

2.3. Monte Carlo simulations

Simulations were performed using the Elekta MLCi head model within PRIMO software (version 0.1.5.1307), available at https://www.primoproject.net.PRIMO supports simulation of various Elekta linac models, including the SLi Plus, Axesse, Affinity, Synergy, and Precise, all corresponding to the Elekta MLCi configuration (Brualla et al., 2013).

An Intel(R) Core (TM) i7-1065G7 CPU with 8 GB RAM was employed for all calculations. The PHSP file for the Elekta Axesse accelerator was generated at the exit of the accelerator head using 10^8 particles. PRIMO's suggested default energy parameters for the 6 MV photon beam configuration (ie. 6.5 MeV with 0.25 MeV FWHM) were applied across all three field sizes: 2×2 cm^2, 4×4 cm^2 and 10×10 cm^2 (Marzon, 2024). Each simulation required approximately two weeks to complete, and splitting roulette was used as recommended for energies below 15 MV (Rodriguez et al., 2012).

The generated PHSP files were then imported into penEasy for dose distribution calculations within a water phantom of $60 \times 60 \times 40$ cm^3, with the space between the PHSP file and the water phantom filled with 36.9 cm of air to reproduce the 90 cm SSD from the measurements (see Fig. 1).

In order to reduce statistical uncertainty to approximately 1.5 %, the PHSP files generated with 10^8 histories were reused 50 times with different random seeds, simulating the interaction of a total of 5×10^9 particles interacting in the water phantom, without employing additional variance reduction techniques. The estimation of statistical uncertainties in this study does not account for the latent variance described by Sempau et al. (2001), steming for the reutilization of the same PHSP in the 50 simulations.We estimate that the contribution of latent variance would be small, however, given the reduced size of the irradiation fields, and the initial number of histories in the PHSP.

To accurately capture dose gradients, the voxel size was set to $0.15 \times 0.15 \times 0.34$ cm^3. This high resolution in the x and y dimensions enabled precise modeling of dose variations critical for small-field simulations, while the larger z-axis voxel size optimized processing time without sacrificing spatial accuracy. The 50 simulations of 10^8 histories, were run in parallel on a high capacity cluster, allowing for the completion of the 50 simulations within hours.

OF were calculated from the MC simulations as the ratio between absorbed dose per history calculated at 10 cm depth from each field size, and the absorbed dose calculated for the reference 10×10 cm^2 field at the same depth, mirroring the method used to determine OF values from experimental measurements. The uncertainty of the OF was determined using equation (1) with a method similar to that applied to the experimental data, incorporating an uncertainty factor (k = 2). The uncertainty estimation is expressed as the combined uncertainty, in accordance with the methodology proposed by (Ayala et al., 2024).

2.4. Dosimetric evaluation

The dosimetric evaluation was performed by comparing the simulated and measured output factors, PDDs, transverse profiles and dose maps, when avail-able. For this purpose, relative differences and gamma analysis were used (Low et al., 1998). Gamma analysis was performed with acceptance criteria of 1 mm distance-to-agreement (DTA) and dose differences of 1 %, 2 % and 3 %, with a 10 % threshold. The DTA was restricted to 1 mm to take into account that, in steep dose gradients areas, such as in this case, most points will fail on distance and not on dose (Vidal et al., 2019) (Ibáñez et al., 2021).

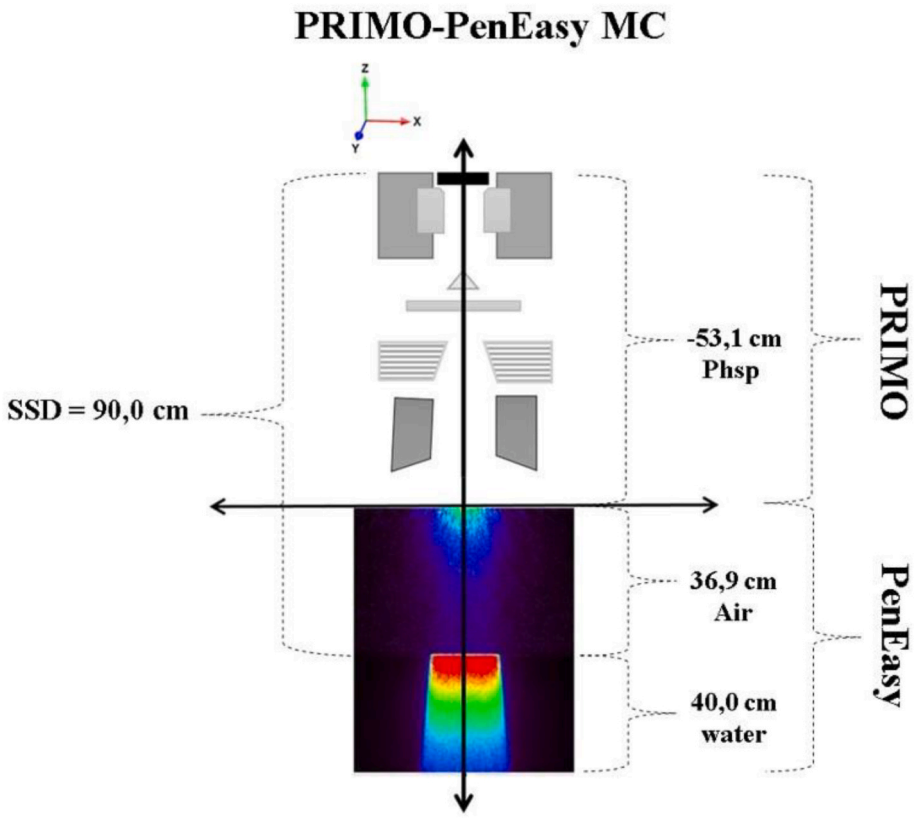

Fig. 1. Sketch of the geometry of LINAC head, simulated with PRIMO in the first phase of the simulation, and the dose calculation in the air-water phantom simulated with penEasy in the second phase.

3. Results

3.1. Percentage depth dose

The percentage depth doses (PDD) obtained with the Semiflex IC were compared to PRIMO-PenEasy MC simulations for three field sizes: $2 \times 2\ cm^2$, $4 \times 4\ cm^2$ and $10 \times 10\ cm^2$. The comparison between the PDDs is shown in Fig. 2, as well as the relative differences. For all field sizes, the largest discrepancies were found within the 0–2 cm depth range, just before reaching the point of maximum ionization, with maximum differences of 4.4 %, 3.4 %, and 3.0 %, for the 2×2 cm^2, 4×4 cm^2 and 10×10 cm^2 field sizes, respectively. This region exhibits a high dose gradient, where ionization chambers with a small cavity volume (0.125 cm^3) are known to overestimate dose values due to the lack of charged particle equilibrium (Delfs et al., 2019). Beyond 2 cm in depth, the differences remained below 2.5 %. The experimental uncertainties of the IC were found to be approximately 1.6 %, and the statistical uncertainty of the simulation was around 1.5 %.

3.2. Dose profiles

A comparative analysis was conducted between dose profiles measured with the IC, EBT3 films, and those obtained from PRIMO-PenEasy simulations. Fig. 3 shows the comparison of the profiles along the crossplane and inplane directions for each field size, as well as with the corresponding gamma values calculated using a 1 %-1 mm gamma index criterion and a 10 % threshold and Fig. 4 show the gamma analysis results for the three dose difference and DTA criteria comparing simulations with experimental data from the IC and EBT3 films.

For the comparison with the EBT3, a gamma evaluation of the 2-dimensional dose maps was also performed and results are shown in Table 1. An example of the $2 \times 2\ cm^2$ field evaluation is also presented in Fig. 5, where isodose profiles measured with EBT3 and simulated at 10 cm depth are represented together, as well as the 2D-1 %-1 mm gamma evaluation.

Radiochromic films generally provide better results in terms of gamma evaluation compared to IC measurements. This trend becomes more pronounced as the field size decreases and the gamma criteria becomes more restrictive. For instance, in the most restrictive gamma and with the smallest field size, the passing rate for radiochromic film measurements exceeds that of the IC by approximately 15 percentage points. This is consistent with the observations from the transverse profiles, where the crossplane and inplane profiles measured with the IC showed larger discrepancies when compared to PRIMO-PenEasy simulations. In contrast, dose profiles measured with EBT3 radiochromic films demonstrated closer alignment with the simulation results.

The non-negligible volume effect of the IC causes a smoothing effect in the dose fall-off, which becomes more apparent as the field size decreases. This effect, however, is not present with radiochromic films, which offer a higher spatial resolution.

3.3. Output factors

Table 2 provides a detailed comparison of the simulated and measured output factors at a depth of 10 cm for each field size, as well as the relative difference and uncertainty. The output factors show a good

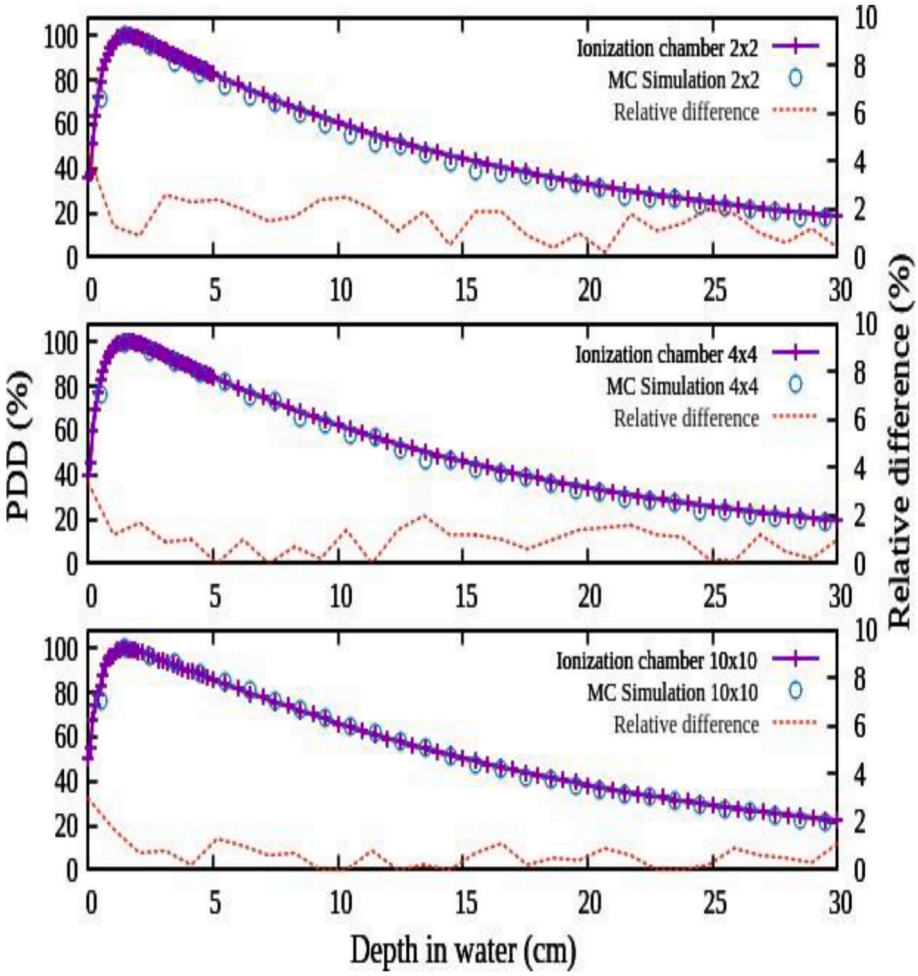

Fig. 2. Measured and simulated PDD and relative differences for field sizes: (a) $2 \times 2\ cm^2$; (b) $4 \times 4\ cm^2$; (b) $10 \times 10\ cm^2$.

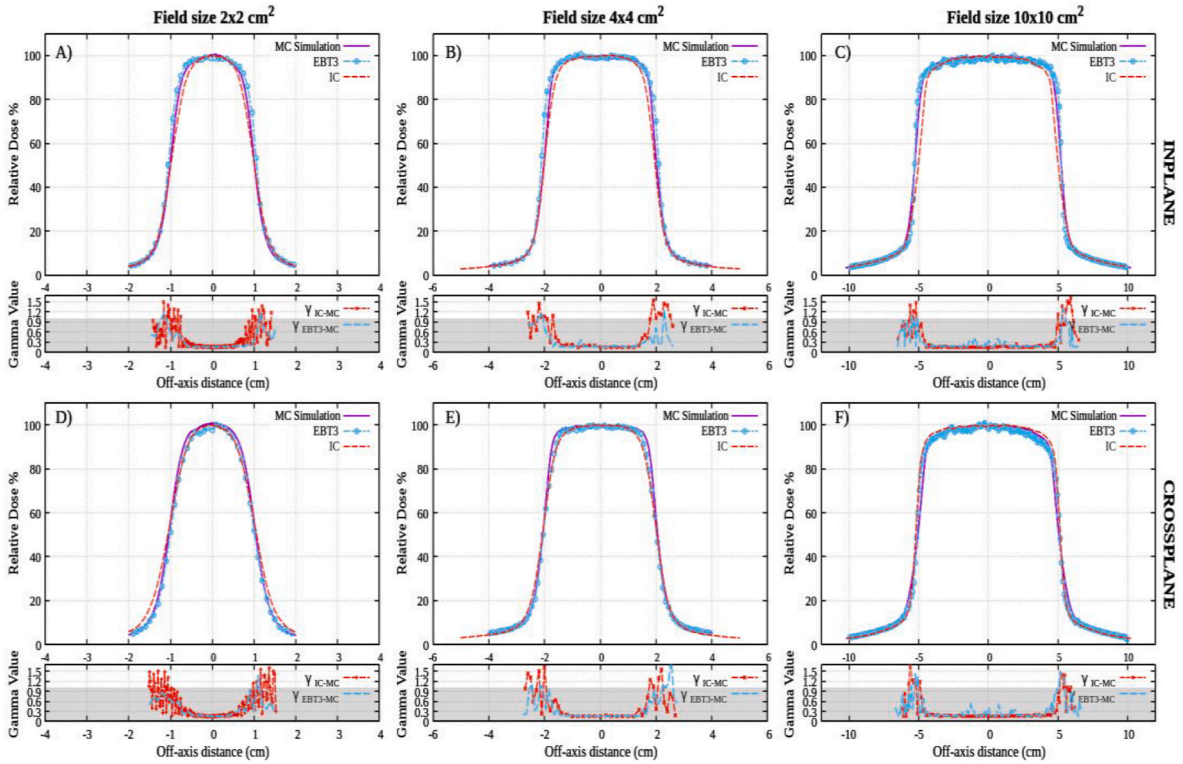

Fig. 3. Comparison of relative dose profiles and gamma evaluation for different field sizes and measurement orientations. Columns correspond to field sizes of 2 × 2 cm^2 (left), 4 × 4 cm^2 (center), and 10 × 10 cm^2 (right). The top row shows In-plane measurements, and the bottom row Cross-plane measurements. Each figure includes a top image comparing relative dose profiles from MC (purple), IC (red), and EBT3 (blue), and a bottom image showing gamma evaluation (1 %-1 mm, 10 % threshold), with red for MC vs. IC and blue for MC vs. EBT3. The shaded area marks regions meeting the gamma criterion.

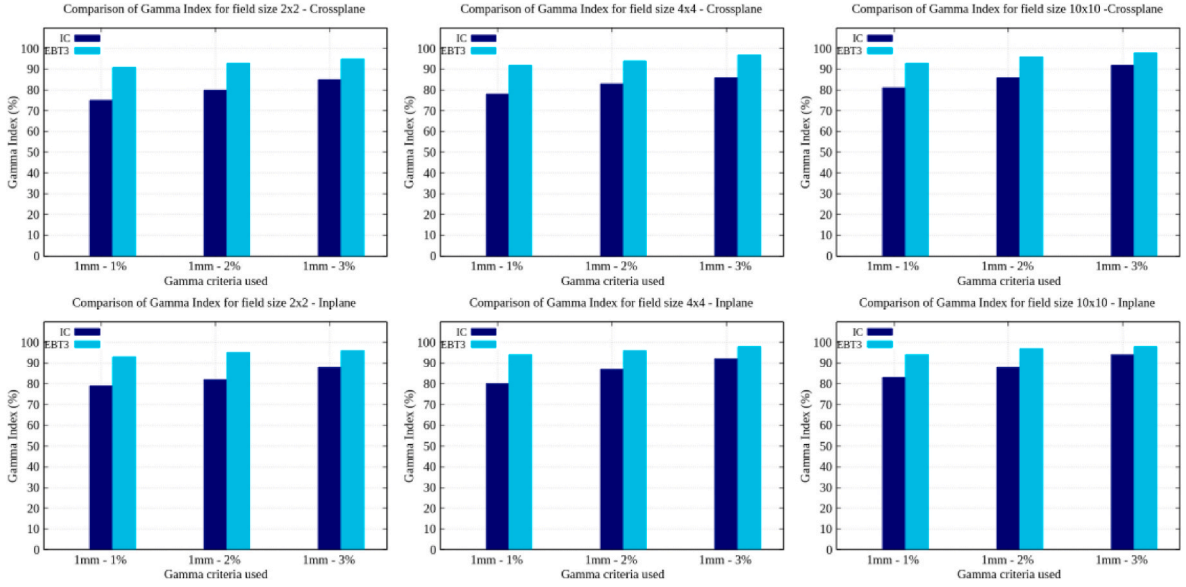

Fig. 4. Percentage of points passing the gamma index between measured and simulated data for the cross-plane (top) and in-plane (bottom) directions across the three field sizes. The light blue columns represent the gamma pass rates between EBT3 film measurements and PRIMO-PenEasy simulations, while the dark blue columns indicate the pass rates for the Semiflex IC com-pared with PRIMO-PenEasy simulations.

agreement between simulations and measurements, with relative differences not exceeding 3.5 %.

The uncertainty of the output factors OF is related to the measurement of the beam profiles in the crossplane and inplane directions and, therefore, to the size of the irradiation field. The deviations in the crossline direction were greater than in the inplane direction for all field sizes, decreasing as the field size increased, which can be associated with the presence of a plateau region in the profiles at larger field sizes. For the 10 × 10 cm^2 field, the deviations were constant, as expected for the reference field.

Finally, the standard deviations associated with the OF ranged from 0.015 to 0.019 and increased as the field size decreased, which is

Table 1
2D Gamma index between radiochromic EBT3 and PRIMO- penEasy MC. Percentage of points passing the test.

2D Gamma Index Results			
Field Size (cm^2)	1 mm, 1 %	1 mm, 2 %	1 mm, 3 %
2 × 2	90 %	94 %	96 %
4 × 4	93 %	95 %	98 %
10 × 10	94 %	97 %	98 %

reflected in the final uncertainty.

4. Discussion

Small photon beam dosimetry presents a range of challenges due to the unique characteristics of small fields, including steep dose gradients, partial source occlusion, and lateral electronic disequilibrium. These factors complicate dose measurements and underscore the need for precise instrumentation and methodologies. This study evaluated PRIMO-PenEasy simulations in combination with experimental data obtained using the PTW 31010 Semiflex ionization chamber and EBT3 radiochromic films to address these challenges.

The results highlight the strengths and limitations of each approach and provide evidence for PRIMO-PenEasy's potential as a robust tool for small field dosimetry.

The PTW 31010 Semiflex ionization chamber, commonly used in clinical practice, was evaluated for its performance in small fields. While the ionization chamber produced reasonable results in the equilibrium region of PDD curves, discrepancies emerged in high-gradient regions near the surface and in lateral dose profiles. The chamber's 0.125 cm^3 sensitive volume averages dose values, causing smoothing effects that are particularly pronounced in small fields such as 2 × 2 cm^2. These effects were evident in the gamma analysis, where the ionization chamber achieved a minimum pass rate of 75 % under the 1 %-1 mm criteria.

The observed discrepancies agree with findings from previous studies, such as Ardila et al. (Ardila, 2000), which recommended smaller detectors like the PTW 31016 pinpoint 3D chamber or the PTW 60017 E-diode for small field measurements. Such detectors offer improved spatial resolution and reduce the averaging effects inherent in larger chambers.

In contrast, EBT3 radiochromic films provided better spatial resolution, allowing for more accurate measurements of dose gradients and penumbra regions. The films demonstrated a better agreement with PRIMO-PenEasy simulations, achieving a minimum gamma pass rate of 91 % under the most restrictive 1 %-1 mm criteria. This superior performance highlights the utility of EBT3 films for capturing fine details in small field dosimetry. Their close alignment with PRIMO-PenEasy results further validates the reliability of both methods for small field dosimetry.

PRIMO-PenEasy simulations showed strong agreement with experimental measurements across all evaluated parameters, including PDD, dose profiles, and output factors. For PDD, discrepancies between PRIMO-PenEasy and experimental measurements were most pronounced in the surface region (0–2 cm depth), where high dose gradients occur, with maximum differences of 4.4 % for the smallest field size. Beyond this region, differences remained below 2.5 %. The simulations also provided reliable output factors, with relative differences not exceeding 3.5 % compared to experimental values.

The gamma analysis of lateral dose profiles further supported PRIMO PenEasy's precision, demonstrating high pass rates when compared with EBT3 film measurements.

These results are consistent with previous studies that have validated PRIMO-PenEasy for small field applications. For instance, Gonzales et al. (Gonzalez-Lopez et al., 2015b) and Sarin et al. (2020) demonstrated strong agreement between PRIMO simulations and experimental data, confirming its reliability for simulating medical linear accelerators, including those from Elekta and Varian.

The findings of this study have significant implications for clinical practice. The limitations of ionization chambers in small field dosimetry highlight the importance of integrating high-resolution detectors like EBT3 films with advanced simulation tools. The complementary use of PRIMO- PenEasy and EBT3 films allows for a more accurate characterization of small fields, improving the precision of treatment planning and dose delivery in radiotherapy.

PRIMO-PenEasy's versatility, including its ability to model various field sizes and configurations, makes it a valuable resource for addressing discrepancies in dosimetry across different detectors. Its application extends beyond small fields to include other specialized treatment scenarios, such as intensity-modulated radiation therapy (IMRT).

Based on the results of this study, we recommend using PRIMO-PenEasy for small field dosimetry. This MC code provides a reliable approach for vali-dating dose distributions and resolving discrepancies observed with ionization chamber measurements.

Table 2
Comparison of simulated and measured output factor (OF) values for different field sizes at 10 cm depth.

Field Size (cm2)	Semiflex IC	PRIMO-penEasy MC	Relative difference (%)
2 × 2	0.797 ± 0.017	0.784 ± 0.035	1.6
4 × 4	0.879 ± 0.015	0.848 ± 0.033	3.5

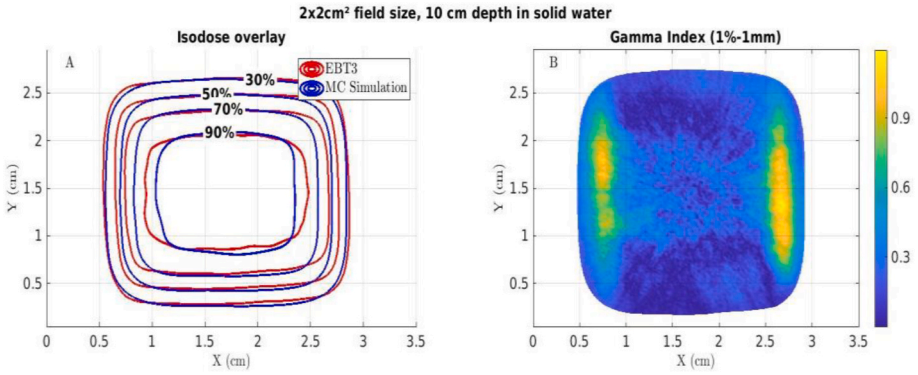

Fig. 5. a) Isodose contours for the 2 × 2 cm^2 obtained from the EBT3 mea-surements (red) and from the MC simulation (blue) and b), the corresponding 1 %-1 mm gamma index map.

5. Conclusions

This study demonstrates that PRIMO-PenEasy is a powerful tool for small field dosimetry, capable of addressing the limitations of traditional mea-surement methods and improving the precision of radiotherapy treatment planning.

Future research should explore the application of PRIMO-PenEasy to a wider range of field sizes and treatment configurations, including irregular and non-symmetrical fields. Additional studies could also investigate the inte-gration of PRIMO-PenEasy into clinical workflows, focusing on optimizing simulation times and incorporating advanced detector technologies for even greater accuracy.

CRediT authorship contribution statement

Nataly Díaz: Writing – review & editing, Writing – original draft, Validation, Software, Methodology, Formal analysis, Data curation, Conceptualization. **Amaia Villa Abaunza:** Methodology. **Jorge Muñoz:** Supervision. **José Manuel Udías:** Writing – review & editing, Supervision, Resources, Conceptualization. **Paula Ibáñez:** Writing – review & editing, Supervision, Formal analysis, Conceptualization.

Ethics approval and consent to participate

Not applicable.

Consent for publication

Not applicable.

Data availability:

All data generated or analyzed during this study are included in this published article [and its supplementary information files].

Funding

There are no available sources of financing.

Declaration of competing interest

The authors declare that they have no known competing financial interests or personal relationships that could have appeared to influence the work reported in this paper.

Acknowledgements

This work was funded by the Spanish Government under the project (PID2022-137114OA-I00 INVENTOR), as well as by the Comunidad de Madrid under the project “Tecnologías Avanzadas para la Exploracio’n del Universo y sus Componentes” (PR47/21 TAU), by the Recovery, Transforma-tion, and Resilience Plan from the Spanish State, and by NextGenerationEU from the European Union through the Recovery and Resilience Facility.

This contribution is for the Moncloa Campus of International Excellence, “Nuclear Physics Group-UCM,” Ref. 910059. Part of the calculations for this work were performed on the “Computing Cluster for Physical Techniques,” funded partially by UCM and partially by EU Regional Funds.

Data availability

Data will be made available on request.

References

Almond, P.R., Biggs, P.J., Coursey, B.M., Hanson, W.F., Huq, M.S., Nath, R., Rogers, D.W. O., 1999. Aapm’s tg-51 protocol for clinical reference dosimetry of high-energy photon and electron beams. Med. Phys. 26. https://doi.org/10.1118/1.598691.

Ardila, I.D., 2000. Dosimetría de campos pequeños de fotones en el contexto de tratamiento de radiocirugía estereostática intracraneal(srs). M.S. thesis. Pontificia Universidad Javeriana.

Aspradakis, M., Byrne, J., Palmans, H., 2010. Ipem Report Number 103: Small Field Mv Photon Dosimetry. Institute of Physics and Engineering in Medicine.

Ayala, R., García, R., Ruiz, G., García, M.J., Soza, Gómez, S., Udías, J.M., Ibáñez, P., 2024. Dosimetric study of bevel factors in ioert with mobile linacs: towards a unified code of practice. Phys. Med. 127, 104836. https://doi.org/10.1016/j.ejmp.2024.104836.

Baro, J.M.F., Sempau, V.J., Salvat, F., 1995. Penelope: an algorithm for Monte Carlo simulation of the penetration and energy loss of electrons and positrons in matter no. 483. Nucl. Instrum. Methods Phys. Res. Sect. B Beam Interact. Mater. Atoms 45, 31–46. https://doi.org/10.1016/0168-583X(95)00349-5.

Brualla, L., Rodriguez, M., Sempau, J., 2013. PRIMO Quick Start Guide. Universität Duisburg-Essen, Universitätsklinikum Essen, NCTeam,Strahlenklinik, Germany; Universitat Politecnica de Catalunya. Institutde Tècniques Energètiques, Spain.

Butson, M.J., Cheung, T., Yu, P.K.N., 2006. Weak energy dependence of ebt gafchromic film dose response in the 50 kvp-10 mvp x-ray range. Appl. Radiat. Isot. 64, 60–62. https://doi.org/10.1016/j.apradiso.2005.07.002.

Castellano, G., Brusa, D., Carrara, M., Gambarini, G., Valente, M., 2007. An optimized Monte Carlo (penelope) code for the characterization of gel-layer detectors in radiotherapy. Nucl. Instrum. Methods Phys. Res. Sect. A Accel. Spectrom. Detect. Assoc. Equip. 580, 502–505. https://doi.org/10.1016/j.nima.2007.05.215.

Cheng, C.W., Cho, S.H., Taylor, M., Das, I.J., 2007. Determination of zero field size percent depth doses and tissue maximum ratios for stereotactic radiosurgery and imrt dosimetry: comparison between experimental measurements and Monte Carlo simulation. Med. Phys. 34, 3149–3157. https://doi.org/10.1118/1.2750968.

Chiu-Tsao, S.T., Ho, Y., Shankar, R., Wang, L., Harrison, L.B., 2005. Energy dependence of response of new high sensitivity radiochromic films for megavoltage and kilovoltage radiation energies. Med. Phys. 32, 3350–3354. https://doi.org/10.1118/1.2065467.

Das, I.J., Ding, G.X., Ahnesjö, A., 2008. Small fields. Nonequilibrium Radiationdosimetry. https://doi.org/10.1118/1.2815356.

Delfs, B., Kapsch, R.P., Chofor, N., Looe, H.K., Harder, D., Poppe, B., 2019. A new reference-type ionization chamber with direction-independent response for use in small-field photon-beam dosimetry – an experimental and Monte Carlo study. Zeitschrift fur Medizinische Physik 29, 39–48. https://doi.org/10.1016/j.zemedi.2018.05.001.

Devic, S., Seuntjens, J., Hegyi, G., Podgorsak, E.B., Soares, C.G., Kirov, A.S., Ali, I., Williamson, J.F., Elizondo, A., 2004. Dosimetric properties of improved gafchromic films for seven different digitizers. Med. Phys. 31, 2392–2401. https://doi.org/10.1118/1.1776691.

Devic, S., Tomic, N., Lewis, D., 2016. Reference radiochromic film dosimetry: review of technical aspects. Phys. Med. 32 (4), 541–556. https://doi.org/10.1016/j.ejmp.2016.02.008.

Dufreneix, S., Bellec, J., Josset, S., Vieillevigne, L., 2021. Field output factors for small fields: a large multicentre study. Phys. Med. 81, 191–196. https://doi.org/10.1016/j.ejmp.2021.01.001.

Efendi, M.A., Funsian, A., Chittrakarn, T., Bhongsuwan, T., 2020. Monte Carlo simulation using primo code as a tool for checking the credibility of commissioning and quality assurance of 6 mv truebeam stx varian linac. Rep. Practical Oncol. Radiother. 25, 125–132. https://doi.org/10.1016/j.rpor.2019.12.021.

Esposito, A., Silva, S., Oliveira, J., Lencart, J., Santos, J., 2018. Primo software as a tool for Monte Carlo simulations of intensity modulated radiotherapy: a feasibility study. Radiat. Oncol. 13, 91. https://doi.org/10.1186/s13014-018-1021-2.

Ezzell, G.A., Burmeister, J.W., Dogan, N., Losasso, T.J., Mechalakos, J.G., Mihailidis, D., Molineu, A., Palta, J.R., Ramsey, C.R., Salter, B.J., Shi, J., Xia, P., Yue, N.J., Xiao, Y., 2009. Imrt commissioning: multiple institution planning and dosimetry comparisons, a report from aapm task group. Med. Phys. 36, 5359–5373. https://doi.org/10.1118/13238104.

Francescon, P., Cora, S., Cavedon, C., Scalchi, P., Reccanello, S., Colombo, F., 1998. Use of a new type of radiochromic film, a new parallelplate micro- chamber, mosfets, and tld 800 microcubes in the dosimetry of small beams. Med. Phys. 25, 503–511. https://doi.org/10.1118/1.598227.

Gonzalez-Lopez, A., Vera-Sanchez, J.A., Lago-Martin, J.D., 2015a. Small fields measurements with radiochromic films. J. Med. Phys. 40, 61–67. https://doi.org/10.4103/0971-6203.158667.

Gonzalez-Lopez, A., Vera-Sanchez, J.A., Lago-Martin, J.D., 2015b. Small fields measurements with radiochromic films. J. Med. Phys. 40, 61–67. https://doi.org/10.4103/0971-6203.158667.

Ibáñez, P., Villa-Abaunza, A., Vidal, M., Guerra, P., Graullera, S., Illana, C., Udías, J.M., 2021. XIORT-MC: a real-time MC-based dose computation tool for low-energy X-rays intraoperative radiation therapy. Med. Phys. 48 (12), 8089–8106. https://doi.org/10.1002/mp.15291.

Leksell, L., 1983. Occasional review stereotactic radiosurgery. J. Neurol. Neurosurg. Psychiatr. 46. https://doi.org/10.1136/jnnp.46.9.797.

Low, D.A., Harms, W.B., Mutic, S., Purdy, J.A., 1998. A technique for the quantitative evaluation of dose distributions. Med. Phys. 25, 656–661. https://doi.org/10.1118/1.598248.

Marzon, J.R.L., 2024. Validation of the elekta synergy platform linac at 6 mv photon beam using primo Monte Carlo software. J. Med. Phys. 49 (3), 410–418. https://doi.org/10.4103/jmp.jmp4824.

McNiven, A.L., Mulligan, M., Kron, T., Battista, J.J., 2006. The response of prototype plane-parallel ionization chambers in small megavoltage x-ray fields. Med. Phys. 33, 3997–4004. https://doi.org/10.1118/1.2356650.

Micke, A., Lewis, D.F., Yu, X., 2011. Multichannel film dosimetry with nonuniformity correction. Med. Phys. 38, 2523–2534. https://doi.org/10.1118/1.3576105.

Palmans, H., Andreo, P., Huq, S., Seuntjens, J., 2017a. Dosimetry of Small Static Fields Used in External Beam Radiotherapy: an Iaea-Aapm International Code of Practice for Reference and Relative Dose Determination, vol. 45. International Atomic Energy Agency, pp. 1123–1145. https://doi.org/10.1002/mp.13208. Technical report series no. 483.

Palmans, H., Andreo, P., Huq, S., Seuntjens, J., 2017b. Dosimetry of small static fields used in external beam radiotherapy: an iaea-aapm international code of practice for reference and relative dose determination. Technic. Rep. Ser. No. 483 45, 1123–1145. https://doi.org/10.1002/mp.13208.

Rodriguez, M., Sempau, J., Brualla, L., 2012. A combined approach of variance-reduction techniques for the efficient Monte Carlo simulation of linacs. Phys. Med. Biol. 57, 3013–3024. https://doi.org/10.1088/00319155/57/10/3013.

Rodriguez, M., Sempau, J., Brualla, L., 2013. Primo: a graphical environment for the Monte Carlo simulation of varian and elekta linacs. Strahlenther. Onkol. 189, 881–886. https://doi.org/10.1007/s00066-013-0415-1.

Sánchez-Doblado, F., Andreo, P., Capote, R., Leal, A., Perucha, M., Arráns, R., Núñez, L., Mainegra, E., Lagares, J.I., Carrasco, E., 2003. Ionization chamber dosimetry of small photon fields: a Monte Carlo study on stopping-power ratios for radiosurgery and imrt beams. Phys. Med. Biol. 48, 2081–2099. https://doi.org/10.1088/0031-9155/48/14/304.

Sarin, B., Bindhu, B., Saju, B., Nair, R., 2020. Validation of primo Monte Carlo model of clinac ix 6mv photon beam. J. Med. Phys. 45, 24–35. https://doi.org/10.4103/jmp.JMP7519.

Sempau, J., Sánchez-Reyes, A., Salvat, F., Tahar, H., Jiang, S.B., Fernández-Varea, J.M., 2001. Monte Carlo simulation of electron beams from an accelerator head using penelope. Phys. Med. Biol. 46 (4), 1163–1186. https://doi.org/10.1088/0031-9155/46/4/318.

Sempau, J., Badal, A., Brualla, L., 2011. A penelope-based system for the automated Monte Carlo simulation of clinacs and voxelized geometries application to far-from-axis fields. Med. Phys. 38, 5887–5895. https://doi.org/10.1118/1.3643029.

Vera, J.A., 2018. Estudio del ruido y análisis de la incertidumbre en dosimetría con película radiocromica. Ph.D. thesis. Universidad de Granada.

Vidal, M., Ibánez, P., Guerra, P., Valdivieso-Casique, M.F., Rodriguez, R., Illana, C., Udias, J.M., 2019. Fast optimized Monte Carlo phase-space generation and dose prediction for low energy x-ray intra-operative radiation therapy. Phys. Med. Biol. 64, 075002. https://doi.org/10.1088/1361-6560/ab03e7.